

# **Fabrication of Titanium Dioxide Nanotubes as Implantable Drug Delivery Systems**

## **Abstract**

Titanium dioxide nanotubes have numerous applications, including dental and orthopedic implants, solar cells, and water purification. The use of titanium metal is prevalent due to its high biocompatibility within the human body. Titanium-based alloys not only exhibit excellent corrosion resistance in bodily environments but also demonstrate compatibility with human tissues, particularly bones. This project aims to fabricate titanium dioxide nanotubes using anodizing techniques for drug delivery in orthopedic implants. The objective is to provide valuable insights into targeted drug delivery, minimizing the non-targeted consumption of medication by patients. Antibiotics will be loaded into the nanotubes for controlled release. A biocompatible polymer will be applied to the nanotubes to regulate the drug release rate. Results will be obtained through various analyses, including X-ray diffraction (XRD), scanning electron microscopy (SEM), energy-dispersive X-ray spectroscopy (EDS), infrared spectroscopy (FTIR), nuclear magnetic resonance (NMR), and biological tests.

**Keywords:** Titanium Dioxide, Orthopedic Implants, Anodizing, Drug Delivery, Biocompatible Polymer

Contents	Page
Abstract .....	1
1. Introduction.....	3
2. Materials and Methods.....	4
2.1 Materials Used .....	4
2.2 Laboratory Equipment .....	4
2.3 Anodizing Process.....	4
2.3.1 Sanding .....	4
2.3.2 Polishing .....	4
2.3.3 Degreasing .....	4
2.3.4 Preparation of Coating Solution.....	4
2.3.5 Anodizing Reaction.....	4
2.4 Drug Loading and Release Control.....	4
2.4.1 Preparation of Specific Concentrations for Calibration Curve .....	4
2.4.2 Obtaining the Calibration Curve.....	5
2.4.3 Drug Loading and Release.....	7
2.4.4 Drug Release Timing Control and Evaluation .....	7
2.4.5 PLGA Copolymer Coating Method .....	7
3. Results and Discussion .....	8
3.1 Morphological Study .....	8
3.2 Structural Analysis .....	9
3.3 Drug Release Profile .....	10
4. Conclusion .....	13
5. References.....	13

# 1. Introduction

The development of medical implants for treating fractures and bone deficiencies has always been of great importance. The demand for implants has significantly increased over the past decade, and it is projected to multiply several times by 2030. This increasing need has resulted in a stronger focus on developing more durable implants. Previously, orthopedic implants were made from silver and gold, which were recognized as biocompatible materials, yet their high cost and poor mechanical properties were limitations. The use of metallic alloys became common in this field to overcome these mechanical deficiencies while reducing costs. However, significant challenges, such as rapid corrosion in the human body, persisted [1].

Titanium-based alloys have emerged as the most widely used materials in orthopedic implants due to their favorable physical properties and biocompatibility. Unfortunately, they remain biologically inert and cannot resist infections, making infection related to prosthetics one of the main causes of implant failure. To prevent bacterial infections, antibacterial drugs must be utilized at the implantation site. These drugs can be released smartly and target-specific over time, preventing localized infections at the implanted site. In this project, antibacterial drugs are incorporated within titanium nanostructures, providing an ideal storage solution within the body [2].

Targeted drug delivery is now a critical topic in biomedical engineering. Titanium nanostructures play a significant role in medical applications and drug delivery, as they allow for drug loading and increased surface contact. Various drug-loading methods can significantly affect the volume of drugs encapsulated within the nanotubes. Moreover, these drug-carrying nanotubes, due to their unique properties, can serve as optimal options for implantation to reduce localized infections of the implants [3].

## **2. Materials and Methods**

### **2.1 Materials Used**

The materials used include lactic acid, glycolic acid, diethyl ether, chloroform, silicone oil, absolute ethanol, tin (II) chloride (dihydrate), ethylene glycol, water and titanium grade 23 (Ti-6Al-4V) was utilized.

### **2.2 Laboratory Equipment**

A list of laboratory equipment used in the research includes Vacuum pump, Oven, Magnetic stirrer, Digital thermometer, Laboratory pipette, Balance

### **2.3 Anodizing Process**

The anodizing process involved several steps:

#### **2.3.1 Sanding**

Mechanical sanding was used to remove coarse oxides from the surface of the samples.

#### **2.3.2 Polishing**

The samples were polished to achieve a smooth surface.

#### **2.3.3 Degreasing**

Samples were placed in an ultrasonic bath for 10 minutes to remove surface contaminants.

#### **2.3.4 Preparation of Coating Solution**

A solution containing ethylene glycol and ammonium fluoride was prepared for the anodizing process.

#### **2.3.5 Anodizing Reaction**

The titanium samples were subjected to an anodizing reaction to form titanium dioxide nanotubes.

### **2.4 Drug Loading and Release Control**

#### **2.4.1 Preparation of Specific Concentrations for Calibration Curve**

To prepare specific concentrations for the calibration curve, the solution obtained in the previous step needs to be diluted. For this purpose, the solution is diluted with phosphate buffer in varying volumes to achieve different points for the calibration graph. The initial drug concentration is shown alongside the different amounts of diluted solution in (Table 2.1).

Table 2.1 Table of final drug concentration with phosphate salt

Concentration of initial drug solution	Volume of diluted solution with phosphate salt	Final concentration
0.005 g cc <sup>-1</sup>	10 cc	500 µg/Lit
0.005 g cc <sup>-1</sup>	20 cc	250 µg/Lit
0.005 g cc <sup>-1</sup>	30 cc	166.67 µg/Lit
0.005 g cc <sup>-1</sup>	40 cc	125 µg/Lit
0.005 g cc <sup>-1</sup>	50 cc	100 µg/Lit
0.005 g cc <sup>-1</sup>	60 cc	83.3 µg/Lit
0.005 g cc <sup>-1</sup>	70 cc	71.4 µg/Lit
0.005 g cc <sup>-1</sup>	80 cc	62.5 µg/Lit
0.005 g cc <sup>-1</sup>	90 cc	55.5 µg/Lit
0.005 g cc <sup>-1</sup>	100 cc	50 µg/Lit

## 2.4.2 Obtaining the Calibration Curve

The absorbance at each wavelength for each concentration was measured separately, with a peak noted at 283 nanometers during UV-Visible spectrophotometric testing.

We will plot all the values on a graph and draw it. It is important to note that we set the origin of the graph at the point (0,0) and plot the graph without extending along the X-axis. (Figure 2.2) shows the calibration curve as concentration based on absorbance. Additionally, (Figure 2.1) indicates the highest peak wavelength at the point 283 nm, which we use to measure all samples in relation to this wavelength.

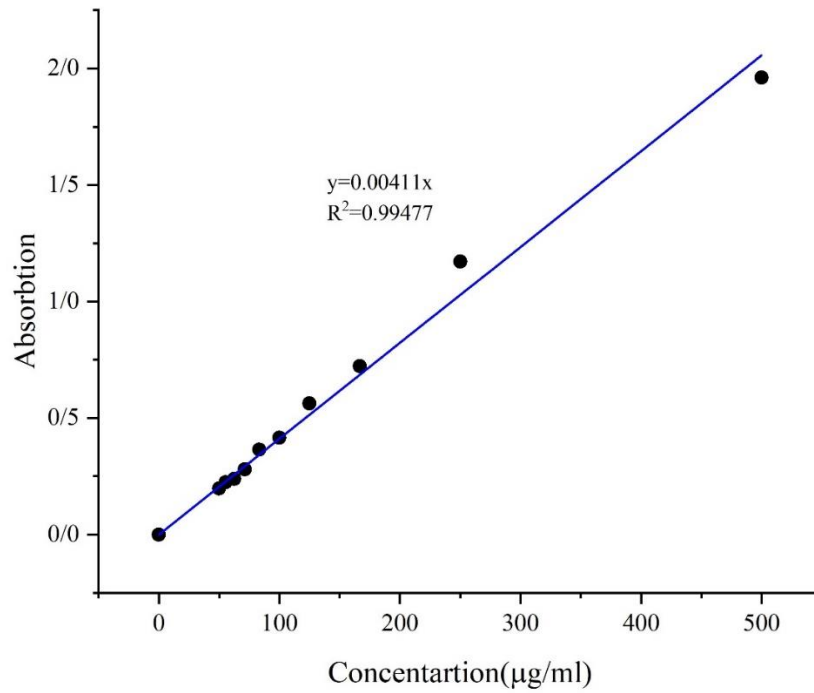


Figure 2.1 Concentration calibration chart based on absorption

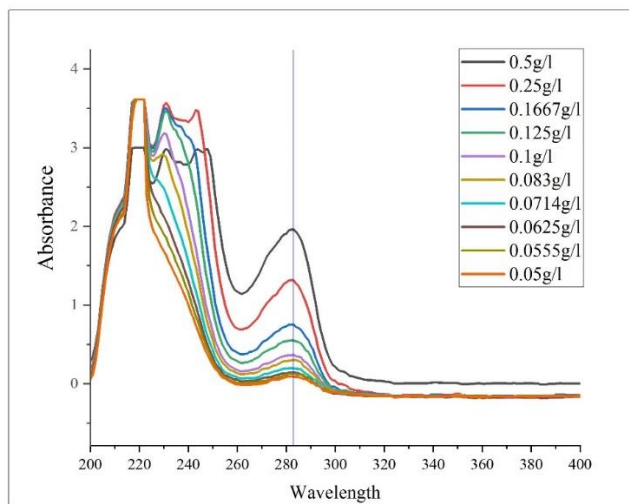


Figure 2.2 Wavelength diagram based on absorption

### 2.4.3 Drug Loading and Release

In this project, various methods were employed for drug loading into titanium nanotubes, and the results were analyzed and evaluated separately. The results from electron microscopy tests for both physical adsorption and electrodeposition methods will be discussed in the next chapter.

#### 2.4.3.1 Physical Adsorption Method

The first method for drug loading onto titanium nanotubes involved physical adsorption. Initially, a drug solution containing the drug and phosphate buffer was prepared and placed into a micropipette. The samples were washed gently with water and prepared for drug loading. Subsequently, 20 microliters of the solution were applied to the samples, allowing time for the drug to penetrate the nanotubes. This process was repeated six times with additional application of the drug solution. A challenge encountered during this method was the formation of deposits on the titanium nanotubes. Due to the negative surface charge of the nanotubes and the positive magnetic charge of the vancomycin drug, reactive interactions caused the formation of sticky deposits. To address this issue, deionized water was utilized instead of the phosphate buffer solution, which resolved the salt precipitation problem and improved drug loading into the nanotubes.

#### 2.4.3.2 Electrodeposition Method

The electrodeposition method relied on the charge differences between the titanium nanotubes and the vancomycin drug. This method created electric cell conditions facilitating the exchange of charges, allowing positively charged vancomycin particles to penetrate the titanium nanotubes upon the application of electric current. In this method, the cathode used was an uncoated titanium sample (Ti6Al4V), and in some tests, graphite served as the cathode. The solution for electrodeposition consisted of deionized water and anhydrous acetic acid with vancomycin, where the drug concentration was 2 grams per liter, and the acid concentration was 1% (v/v). The power supply voltage was set to a constant 10 volts for a duration of 10 minutes.

### 2.4.4 Drug Release Timing Control and Evaluation

For evaluating drug release timing, coated titanium samples were simultaneously prepared for drug loading. After employing the drug loading methods described earlier, the samples were placed in phosphate-buffered saline within different cells. To simulate human body conditions, a temperature of 37 degrees Celsius and a pH of 7.4 were maintained. Titanium samples were removed from the phosphate-buffered saline at specific time intervals for UV-Vis spectroscopic analysis to assess the drug release rate. Each titanium sample was housed in a separate cell to monitor drug release at various times. The rate of drug release from the titanium nanotubes was calculated using a formula derived from the calibration curve obtained for the respective drug.

### 2.4.5 PLGA Copolymer Coating Method

For coating the titanium nanotubes with PLGA copolymer, a polymer solution was prepared by mixing chloroform with the copolymer to create a 1% (w/v) solution. The titanium samples were immersed in the solution for 10 seconds, allowing the polymer to adhere completely. The samples were then dried in an oven at 40 degrees Celsius for 15 minutes.

The results of drug release along with polymer coatings will be presented in the following chapter, along with relevant graphs for analysis.

### 3. Results and Discussion

#### 3.1 Morphological Study

As shown in (Figure 3.1), four images have been taken at different magnifications of the sample. In part (a), the reference titanium sample was photographed to evaluate the surface of uncoated titanium. As observed, the polished and smooth surface of the uncoated titanium sample is evident. In part (b), the coated sample is viewed at a magnification of 50kx. This image clearly shows all the nanotubes formed on the titanium surface. The density of the nanotubes and their significant aggregation at a magnification of 50kx indicates their flawless formation. In part (c), the titanium nanotubes are observed at a magnification of 100kx. The openings of these titanium dioxide nanotubes are seen to be uniform and without surface defects. Additionally, the uniformity in the size of all the openings is quite notable. The diameter of several nanotube openings was measured randomly, resulting in an average opening size of 145 nm. In image (d), further magnification is applied, and we observe at 250kx. A notable point in this image is the measurement of the wall thickness of the nanotubes, which averages around 30 nm. At this magnification, several surface contaminants are also observed around the nanotubes, which can be eliminated with better surface preparation in the samples.

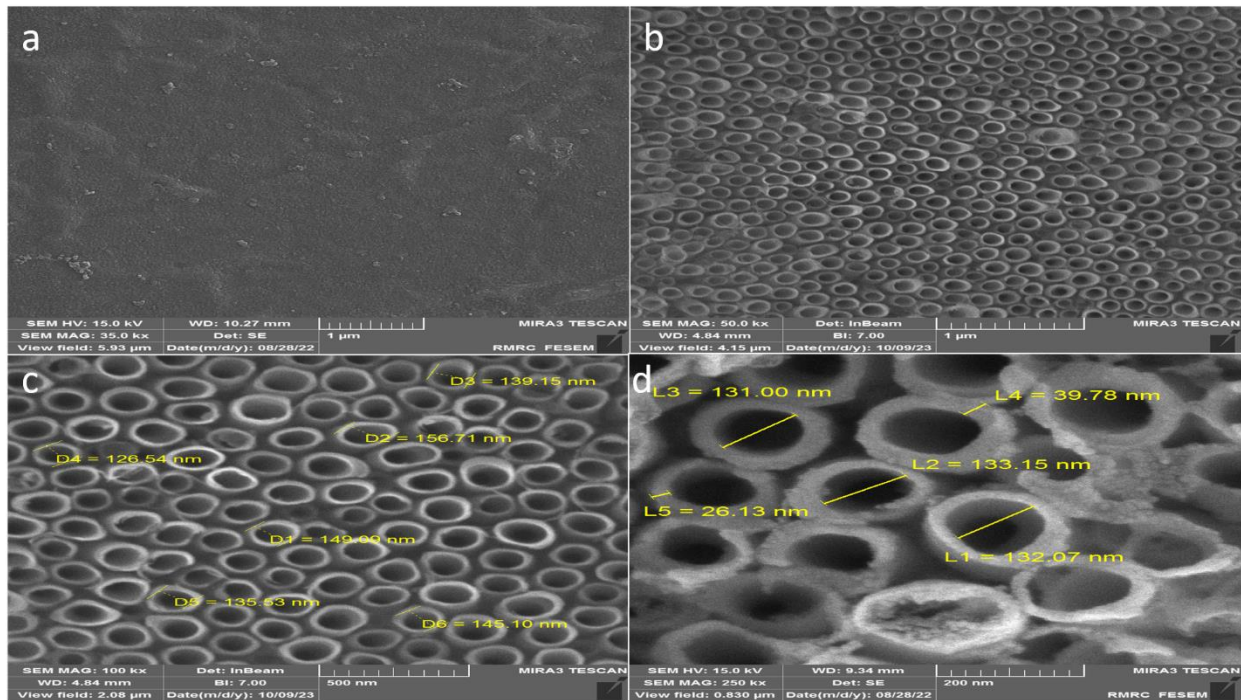


Figure 3.1 FESEM image of titanium nanotubes in different magnifications.

In the next section, we will study the surface morphology of our coated titanium sample from a cross-sectional view. As shown in (Figure 3.2), both images a and b indicate the formation of titanium dioxide in the form of nanotubes. In image a, the average size of the nanotubes is measured and reported as 1.79  $\mu\text{m}$ . Additionally, in image b, we observe the ends of the titanium nanotubes formed on the surface, which appear to be closed.



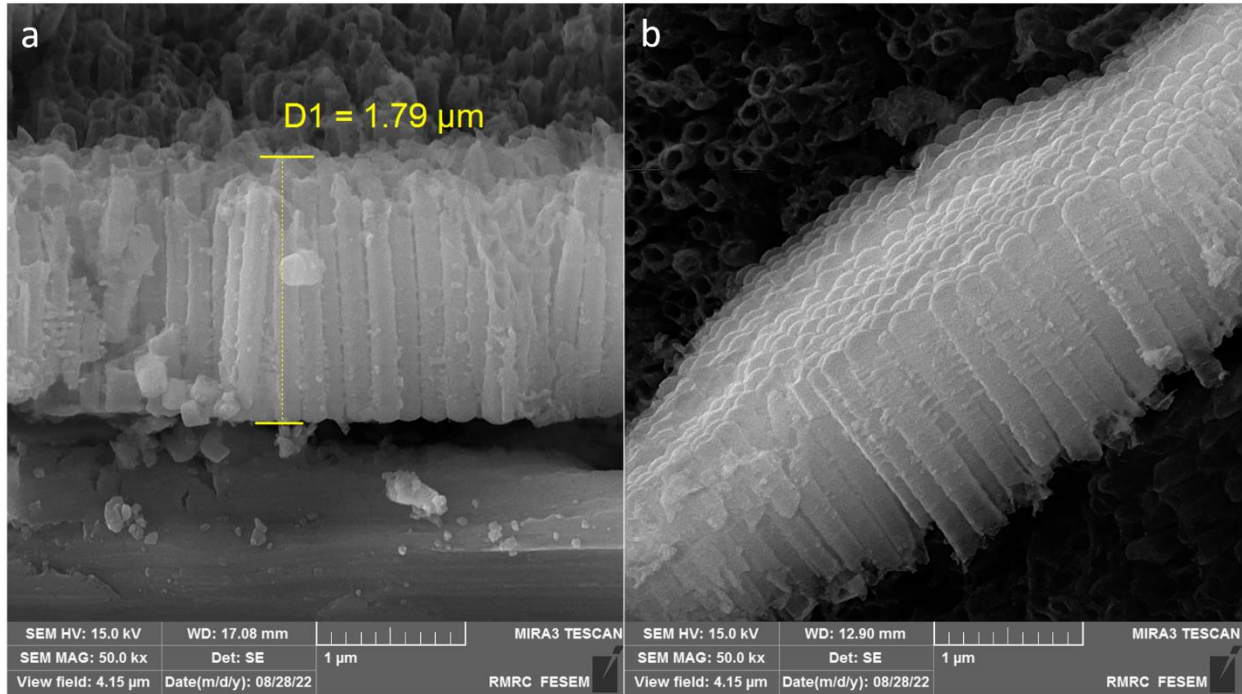


Figure 3.2 Electron microscope image of titanium nanotubes from a cross section

### 3.2 Structural Analysis

We require this analysis to identify and confirm the presence of a coating on our titanium samples. After analyzing the peaks in the graph for the coated samples in comparison to the reference chart of the uncoated sample, we aim to verify the formation of titanium's chemical composition in the oxide and examine the morphology of its anatase phase.

In (Figure 3.3), the X-ray diffraction (XRD) patterns for the Ti6Al4V sample before anodizing, after anodizing, and after annealing are shown. Image a corresponds to the reference sample, image b pertains to the coated sample, and image c is related to the coated sample after thermal treatment in the furnace.

In figure a, the peaks corresponding to titanium are observed at  $2\theta = 35.40, 38.55, 40.46, 53.31, 63.52, 71.00, 74.87, 76.81, 78.07,$  and  $82.58$ , which correspond to the crystal planes (100), (002), (101), (102), (110), (103), (200), (112), (201), and (004), respectively.

As indicated at the beginning of figure b, after anodizing the sample, an amorphous titanium oxide phase has formed on the surface. However, it is noteworthy that not all titanium oxide formed is amorphous; we observe a peak corresponding to the crystalline anatase phase related to the crystal plane (220) at  $2\theta = 71.089$ .

Finally, after annealing the sample at 550 degrees Celsius, we observe the emergence of new peaks related to the anatase phase, which include peaks at  $2\theta = 25.405, 38.086, 48.20,$  and  $54.21$ , corresponding to the crystal planes (101), (004), (200), and (105), respectively.

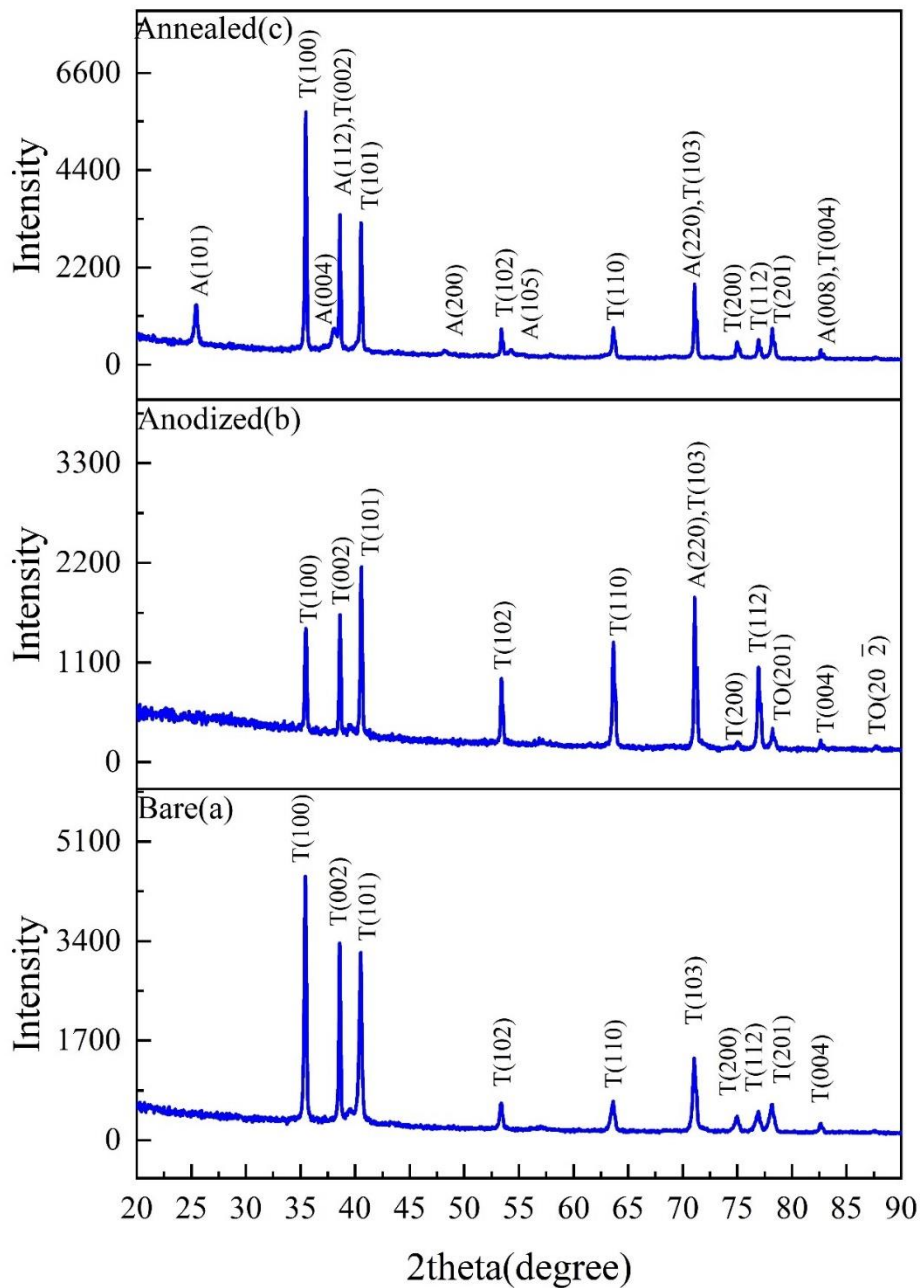


Figure 3.3 X-ray beam diffraction analysis for three different samples

### 3.3 Drug Release Profile

In figures (3.4) and (3.5), we observe drug release tests over a long duration and during the first 6 hours, respectively. Drug release in these delivery systems typically comprises two phases (biphasic release). The first phase is known as burst release, while the second phase involves gradual release. Based on the results

from the first 6 hours, it is evident that using the EPD method, we have been able to partially suppress the burst release in the first phase. This burst release occurs due to the significant concentration difference of the drug between the nanotubes and the release environment. With the EPD method, we managed to reduce the drug concentration from 328.5  $\mu\text{g}/\text{mL}$  to 75.3  $\mu\text{g}/\text{mL}$  after 30 minutes. Furthermore, by analyzing the drug release profile, we observe that the slope of concentration reduction in the EPD method is less steep than that of the physical method. We also successfully increased the release amount during the first 30 minutes to 18  $\mu\text{g}/\text{mL}$  by applying a polymer coating. Using a polymer coating allows for a controlled release mechanism, delivering the drug to infected tissues over a longer period and at appropriate concentrations.

In (Figure 3.4), it can be seen that after about one more day, no drug is released from the sample that was loaded using the physical method. However, in the samples that were loaded using the EPD method and coated with polymer, the drug release continued for several days and was highly controlled. These results indicate that we successfully increased the drug release time and prevented burst release in implantable drug delivery systems, thus reducing the potential for infections resulting from surgery or the excessive use of oral antibiotics.

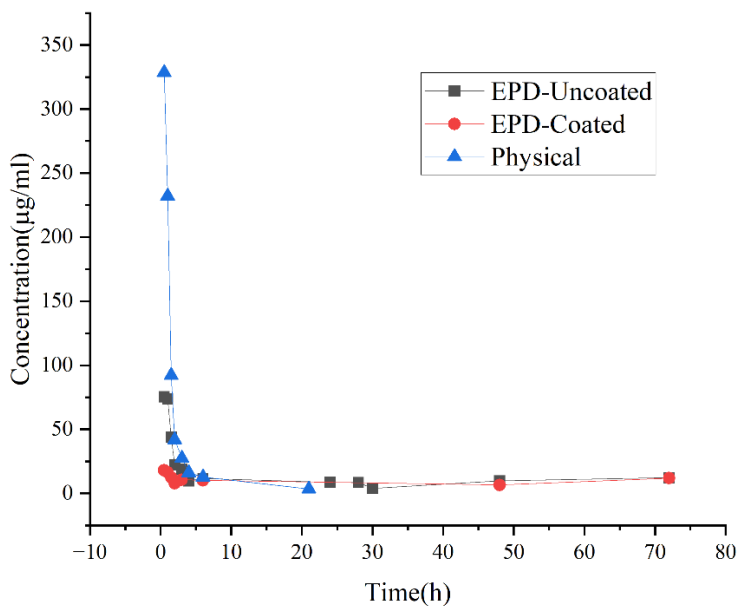


Figure 3.4 Drug release rate diagram of three different samples in the above period of time

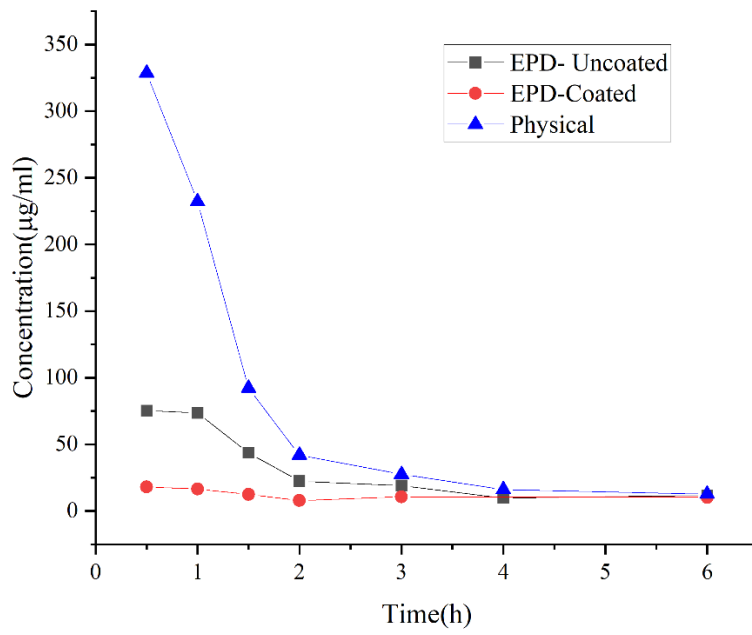


Figure 3.5 Drug release rate diagram of three different samples in six hours

## 4. Conclusion

This study investigates the synthesis and application of titanium dioxide nanotubes as drug delivery systems in orthopedic implants. Utilizing an anodizing process, the nanotubes serve as carriers for controlled and sustained drug release. Results indicate that using polymer coatings and electrophoretic deposition reduces burst release and extends release time, thereby enhancing therapeutic efficacy and reducing postoperative infection risks.

## 5. References

1. Ibrahim, M.Z., et al., *Biomedical materials and techniques to improve the tribological, mechanical and biomedical properties of orthopedic implants–A review article*. Journal of Alloys and Compounds, 2017
2. Li, Y., et al., *Enhanced antibacterial properties of orthopedic implants by titanium nanotube surface modification: a review of current techniques*. International journal of nanomedicine, 2019
3. Jha, R., et al., *Smart carbon nanotubes for drug delivery system: A comprehensive study*. Journal of Drug Delivery Science and Technology, 2020